Functional pattern of brain FDG-PET in amyotrophic lateral sclerosis

Marco Pagani, MD, PhD
Adriano Chiò, MD, FAAN
Maria Consuelo Valentini, MD
Johanna Öberg, PhD
Flavio Nobili, MD
Andrea Calvo, MD, PhD
Cristina Moglia, MD, PhD
Davide Bertuzzo, MD
Silvia Morbelli, MD, PhD
Fabrizio De Carli, Med Phys
Piercarlo Fania
Angelina Cistaro, MD

Correspondence to Dr. Pagani: marco.pagani@istc.cnr.it

ABSTRACT

Objective: We investigated a large sample of patients with amyotrophic lateral sclerosis (ALS) at rest in order to assess the value of ^{18}F-2-fluoro-2-deoxy-D-glucose (^{18}F-FDG) PET as a biomarker to discriminate patients from controls.

Methods: A total of 195 patients with ALS and 40 controls underwent brain ^{18}F-FDG-PET, most within 5 months of diagnosis. Spinal and bulbar subgroups of ALS were also investigated. Twenty-five bilateral cortical and subcortical volumes of interest and cerebellum were taken into account, and ^{18}F-FDG uptakes were individually normalized by whole-brain values. Group analyses investigated the ALS-related metabolic changes. Discriminant analysis investigating sensitivity and specificity was performed using the 51 volumes of interest as well as age and sex. Metabolic connectivity was explored by voxel-wise interregional correlation analysis.

Results: Hypometabolism was found in frontal, motor, and occipital cortex and hypermetabolism in midbrain, temporal pole, and hippocampus in patients with ALS compared to controls. A similar metabolic pattern was also found in the 2 subgroups. Discriminant analysis showed a sensitivity of 95% and a specificity of 83% in separating patients from controls. Connectivity analysis found a highly significant positive correlation between midbrain and white matter in corticospinal tracts in patients with ALS.

Conclusions: ^{18}F-FDG distribution changes in ALS showed a clear pattern of hypometabolism in frontal and occipital cortex and hypermetabolism in midbrain. The latter might be interpreted as the neurobiological correlate of diffuse subcortical gliosis. Discriminant analysis resulted in high sensitivity and specificity in differentiating patients with ALS from controls. Once validated by diseased-control studies, the present methodology might represent a potentially useful biomarker for ALS diagnosis.

Classificaton of evidence: This study provides Class III evidence that ^{18}F-FDG-PET accurately distinguishes patients with ALS from normal controls (sensitivity 95.4%, specificity 82.5%).
Neurology® 2014;83:1067–1074

GLOSSARY

^{18}F-FDG = ^{18}F-2-fluoro-2-deoxy-D-glucose; **ALS** = amyotrophic lateral sclerosis; **BA** = Brodmann area; **CI** = confidence interval; **DA** = discriminant analysis; **FDR_{corr}** = corrected for multiple comparisons with the false discovery rate option; **ROC** = receiver operating characteristic.

Amyotrophic lateral sclerosis (ALS) diagnosis is based on clinical history, neurologic examination, and symptoms progression and is supported by neurophysiologic examination.[1] The role of neuroimaging in ALS is currently limited to the exclusion of other disease processes whose symptoms might explain the clinical and electrophysiologic signs. Despite a large number of studies, only a few biochemical, neurophysiologic, and brain structural investigations have been performed to explore the discriminative value of ALS biomarkers.[2] Recently an MRI study

Supplemental data at Neurology.org

From the Institute of Cognitive Sciences and Technologies (M.P., A. Cistaro), CNR, Rome, Italy; Departments of Nuclear Medicine (M.P.) and Hospital Physics (J.O.), Karolinska Hospital, Stockholm, Sweden; ALS Center (A. Chiò, A. Calvo, C.M., D.B.), "Rita Levi Montalcini" Department of Neuroscience, University of Turin, Italy; Neuroscience Institute of Turin (A. Chiò), Italy; Department of Neuroradiology (M.C.V.), CTO Hospital, Turin, Italy; Clinical Neurology Unit (F.N.), Department of Neurosciences, Ophthalmology and Genetics (DINOGMI) and Department of Health Sciences (S.M.), Nuclear Medicine Unit, Department of Internal Medicine, University of Genoa, Italy; Institute of Molecular Bioimaging and Physiology (F.D.), CNR Genoa Unit, Italy; and Positron Emission Tomography Center IRMET S.p.A. (P.F., A. Cistaro), Euromedic Inc., Turin, Italy.

Go to Neurology.org for full disclosures. Funding information and disclosures deemed relevant by the authors, if any, are provided at the end of the article.

differentiated patients from controls with an accuracy of 90%,[3] although it is often difficult to perform MRI analyses in patients with severe motor and respiratory impairments.

^{18}F-2-fluoro-2-deoxy-D-glucose PET (^{18}F-FDG-PET) measures glucose consumption in the astrocyte-synapse functional unit.[4] It might show reduced glucose utilization in neurodegeneration as well as increased glucose utilization during inflammatory processes.[5]

Besides the reduced ^{18}F-FDG uptake seen in motor areas,[6] the few studies of ^{18}F-FDG-PET performed in patients with ALS have reported frontal lobe,[7] diffuse cortical and basal ganglia,[8] and parietal and occipital cortex[9] hypometabolism. Midbrain hypermetabolism was also recently described by our group.[10] Although these findings support the hypothesis that ALS may be regarded as a multisystem disorder, no study assessed the value of functional imaging in ALS diagnosis.

The aim of the present investigation was 3-fold: (1) to replicate the metabolic changes previously described in a far larger group of patients with ALS; (2) to assess the possible discriminant diagnostic value of ^{18}F-FDG-PET on a volume of interest–based discriminant analysis; and (3) to identify the brain functional connectivity underlying ALS.

METHODS

Participants. A total of 195 patients with ALS (mean age 63.2 years [SD 11.6, range 21–86]; females 78/195) who agreed to undergo ^{18}F-FDG-PET were prospectively recruited between June 2011 and February 2013 at the Turin ALS center. All cases had probable laboratory-supported, probable, or definite ALS according to El Escorial ALS revised criteria.[1] Most patients underwent ^{18}F-FDG-PET within 5 months of diagnosis. Median time between diagnosis and PET examination was 4.1 months (interquartile range = 37–44).

The patients were further classified according to the clinical presentation at the time of PET scan, i.e., spinal (n = 136, mean age 62.5 years [SD 12.6, range 21–86]; females 45/136) and bulbar (n = 59, mean age 64.7 years [SD 10.3, range 42–86]; females 32/59). For this study, we considered bulbar patients to be those with bulbar onset and a loss of less than 4 points on the spinal section of the revised ALS Functional Rating Scale (items 4–12). Fifteen patients (9 with spinal and 6 with bulbar subtype) carried a GGGGCC hexanucleotide repeat expansion in the first intron of the *C9ORF72* gene (≥30 repeats). No statistically significant age difference was found between the 2 subgroups; sex differed at $\chi^2 = 7.70$, $p < 0.01$.

Forty participants (mean age 62 years [SD 14.4, range 27–84]; females 11/40) who were referred to the PET center for a suspected diagnosis of lung cancer in whom no oncologic disease was disclosed with ^{18}F-FDG-PET/CT and who had a normal neurologic assessment served as controls. Exclusion criteria were presence of major systemic illness, major vision disturbances, psychiatric illnesses, and diseases affecting brain functioning and metabolism.[10]

Image acquisition and analysis. Detailed methods were previously described.[10,11] PET/CT scans were acquired by a Discovery ST-E System (General Electric) and images were acquired through 2 sequential scans: CT scan of the brain (thickness of 3.75 mm, 140 kV, 60–80 mA/s) and PET brain scan (1 field of view of 30 transaxial cm). PET scan was initiated immediately after the CT examination in order to use CT data for the attenuation correction of the PET data. Data were collected in 128 × 128 matrices with a reconstructed voxel of 2.34 × 2.34 × 2.00 mm.

We carried out preprocessing and statistical analyses by SPM8-normalizing the images to a customized template obtained using FDG-PET and 3D MRI scans of 40 age-matched healthy controls performed at the same center.[12] Briefly, each FDG-PET scan was first coregistered to the pertinent MRI scan (6 parameters, rigid body transformation) using the coregistration algorithm available in the SPM8 package. Each MRI was then spatially normalized to the SPM8 T1-MRI template using an affine plus nonlinear transformation, and the resulting deformation field was applied to the coregistered FDG-PET scan. The spatially normalized PET images were then averaged to obtain a mean PET image, which was finally smoothed with an 8-mm isotropic Gaussian filter.[13]

We performed group comparisons between controls, patients with ALS, and spinal and bulbar subgroups at a threshold of $p < 0.05$ corrected for multiple comparisons with the false discovery rate option (FDR_{corr}). If significant clusters were found, the more conservative threshold at $p < 0.05$ corrected for multiple comparisons with the familywise error option was also tested. We identified the Brodmann areas (BAs) matching the SPM output to the Talairach coordinates using the subroutine implemented by Matthew Brett (http://brainmap.org/index.html). Finally, we explored the sensitivity, specificity, and accuracy values to distinguish ALS from controls, segmenting 65 BAs in all 235 participants. In order to reduce the number of variables and hence increase the statistical strength of the study, we merged regions with similar anatomo-functional characteristics (i.e., BAs 11 and 47, orbitofrontal cortex; BAs 24 and 32, anterior cingulate cortex; BAs 44, 45, and 46, dorsolateral prefrontal cortex; BAs 1, 2, 3, and 4, somatomotor cortex; BAs 23 and 31, posterior cingulate cortex, amygdala and hippocampus, medial temporal lobe, cortex), resulting in 51 volumes of interest (25 bilaterally and cerebellum). Since we expected that strong asymmetries could characterize pathologic conditions, homologous regions in the opposite hemispheres were considered separately. Discriminant analysis was performed by SPSS (version 19) and generalized linear model analysis. Cross-validation was performed in both analyses. This analysis aims to discriminate patients from controls, providing a Class III level of evidence.

Voxel-wise interregional correlation analysis. The cluster found to be hypermetabolic in patients with ALS compared to controls was saved as a volume of interest. The mean of ^{18}F-FDG uptake values within this volume of interest was computed in the spatially normalized scans of each of the 235 participants and divided by whole-brain counts. These values were covaried with the ^{18}F-FDG uptake values to find regions showing significant voxel-wise correlations at $p < 0.05$ FDR_{corr}. This provided parametric maps of metabolic connectivity across participants.[13]

Standard protocol approvals, registrations, and patient consents. The study design was approved by the institutional ethics committee. Patients and controls signed written informed consent.

RESULTS

Study population. No relevant differences in age and sex were found between patients and controls.

ALS diagnosis was confirmed in all patients at 1-year follow-up.

Group comparison. ***Controls vs ALS.*** Patients with ALS showed 3 large clusters of relative hypometabolism compared to controls at $p < 0.05$ FDR_{corr} (figure 1A, table 1). The clusters included bilateral primary and associative visual cortex and bilateral and premotor cortex, as well as left sensorimotor, frontal eyes field and dorsolateral prefrontal cortex. Large regions with significantly increased metabolism in patients with ALS compared to controls were found in midbrain, bilateral superior temporal gyrus, and hippocampi, bilaterally (figure 1B; table 1).

Controls vs spinal patients. We found a very similar pattern at $p < 0.05$ FDR_{corr} when spinal patients were compared to controls, with hypometabolic clusters in spinal patients in bilateral primary and associative visual cortex and in bilateral prefrontal and premotor cortex. Spinal patients showed a relative hypermetabolism in bilateral midbrain, superior temporal gyrus, and right cerebellum (figure 2, A and B; table e-1 on the *Neurology*® Web site at Neurology.org).

Controls vs bulbar patients. Compared to controls, bulbar patients were relatively hypometabolic at $p < 0.05$ FDR_{corr} in bilateral clusters including motor, premotor, and prefrontal cortex. Only midbrain was relatively hypermetabolic in bulbar patients compared to controls (figure 2, C and D; table e-2).

Bulbar patients vs spinal patients. Compared to spinal patients, bulbar patients showed a relative hypometabolic cluster in left motor and premotor cortex at a statistical threshold of $p_{uncorrected} < 0.001$ at voxel level. The opposite comparison did not show any significant result.

Voxel-wise interregional correlation analysis. In patients with ALS, the midbrain hypermetabolic cluster regressed against ^{18}F-FDG relative uptake in the whole brain significantly correlated at $p < 0.05$ FDR_{corr} (besides the expected autocorrelation in midbrain) with metabolism in cerebellar cortex (cerebellar tonsil, tuber, and pyramid of the vermis and most of the cerebellar lobules) and with the white matter tracts, following the motor fibers of the corona radiata to reach primary motor cortex (figure 3). In controls this correlation was limited to 2 small cerebellar clusters bilaterally.

Discriminant analysis. Following cross-validation, discriminant analysis (DA) resulted in an accuracy of 87.7% (95% confidence interval [CI]: 82.8–91.6) in separating patients and controls, with a sensitivity of 88.7% (CI: 83.4–92.7) and a specificity of 82.5 (CI: 67.2–92.7). The area under the receiver operating characteristic (ROC) curve was 92.9% (CI: 89.7–96.2). The best discrimination was obtained by the generalized linear model analysis using the following volumes of interest: right premotor, left superior

Figure 1 Metabolic differences in controls vs patients with ALS

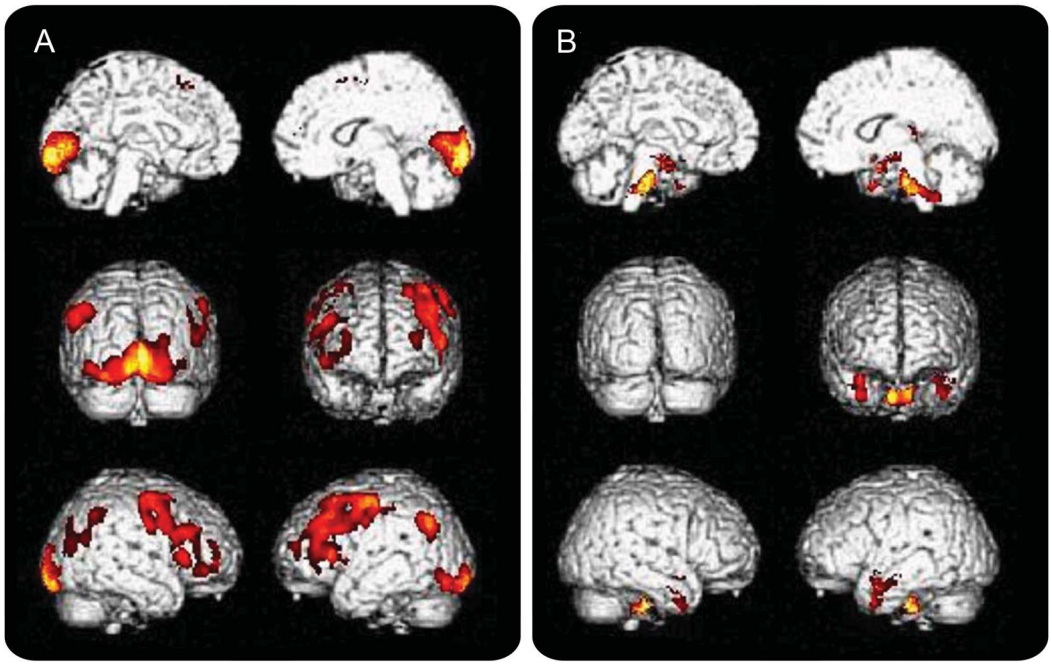

Figure displays regions of significant metabolic differences: (A) hypometabolic regions in amyotrophic lateral sclerosis (ALS); (B) hypermetabolic regions in ALS. Images are color-graded in terms of *z* values. Talairach coordinates and further details are provided in table 1.

Table 1 Results of ^{18}F-FDG brain PET comparison between controls and patients with ALS

	Cluster extent	$pFDR_{corr}$	Maximum *z* score	Region	Talairach coordinates			Cortical region	BA
CTR-ALS	4,011	0.000[a]	6.15	Right occipital	8.0	−90.0	−4.0	Lingual gyrus	17
		0.001[a]	5.78	Right occipital	4.0	−79.0	4.0	Lingual gyrus	18
		0.002[a]	5.61	Left occipital	−4.0	−86.0	−2.0	Lingual gyrus	18
		0.014	5.00	Left occipital	−20.0	−92.0	−6.0	Inferior occipital gyrus	17
	2,604	0.003[a]	5.46	Right frontal	40.0	8.0	36.0	Precentral gyrus	9
		0.004	5.30	Right frontal	38.0	−1.0	52.0	Middle frontal gyrus	6
	3,479	0.003	5.43	Left frontal	−40.0	28.0	24.0	Middle frontal gyrus	46
		0.026	4.84	Left frontal	−42.0	15.0	29.0	Middle frontal gyrus	9
		0.026	4.83	Left parietal	−51.0	−11.0	50.0	Postcentral gyrus	3
		0.026	4.77	Left frontal	−50.0	0.0	42.0	Precentral gyrus	6
		0.029	4.73	Left frontal	−38.0	18.0	49.0	Superior frontal gyrus	8
ALS-CTR	1,174	0.005[a]	5.38	Left temporal	−34.0	−1.0	−15.0	Temporal pole	38
		0.007[a]	5.21	Left temporal	−26.0	−16.0	−11.0	Parahippocampal gyrus	
	1,065	0.005[a]	5.36	Right temporal	38.0	1.0	−22.0	Temporal pole	38
		0.047	4.66	Right cerebrum	38.0	−26.0	−9.0	Caudate	
		0.063	4.51	Right temporal	26.0	−16.0	−9.0	Parahippocampal gyrus	
	823	0.007[a]	5.33	Right cerebrum	8	−24	−38	Midbrain	
		0.047	4.76	Left cerebrum	−6	−22	−34	Midbrain	

Abbreviations: ^{18}F-FDG = ^{18}F-2-fluoro-2-deoxy-D-glucose; ALS = amyotrophic lateral sclerosis (n = 195); BA = Brodmann area; CTR = control (n = 40); $pFDR_{corr}$ = $p < 0.05$ corrected for multiple comparisons with the false discovery rate.
[a] $p < 0.05$ corrected for multiple comparisons with the familywise error.

parietal, bilateral prefrontal, left orbitofrontal, left insular, right primary and associative visual, left temporal, right anterior cingulate, left fusiform, and bilateral parietal cortices, as well as cerebellum, right thalamus, bilateral putamen, and medial temporal lobe, with an accuracy of 93.2% (CI: 89.2–96.5), a sensitivity of 95.4% (CI: 91.4–97.9), and a specificity of 82.5% (CI: 67.2–92.7) (figure 4). The area under the ROC curve was 94.5% (CI: 91.7–97.3) and the difference with DA applied to all 51 volumes of interest was not statistically significant.

DISCUSSION We found highly significant hypometabolism in frontal, premotor, and occipital cortex in 195 patients with ALS compared to controls. The same hypometabolic pattern characterized the spinal subtype, whereas in bulbar patients the analysis showed only frontal and prefrontal hypometabolism, more rostral than spinal patients. Premotor cortex was significantly hypometabolic in all 3 comparisons. In a cohort of patients 6 times as large, this study reproduced the metabolic changes previously found in patients with ALS.[10] Some of the findings, not highlighted in the previous study,[10] are likely the result of the larger sample size and the higher statistical reliability of the present investigation, since the sampling error decreases with the increase of the sample size. The significantly lower frontal metabolism found in the patient groups is not surprising since frontal and prefrontal cortex hypometabolism represents the neurobiological correlate of the cognitive impairment in patients with ALS.[14,15] The hypometabolism found in primary and associative visual cortex is consistent with the extramotor spreading of ALS as described by several surface-based morphometry[16] and diffusion tensor MRI studies,[17,18] showing cortical thinning and decreased fractional anisotropy in these regions, respectively.

Moreover, we confirmed the relative midbrain hypermetabolism in all patient groups and disclosed a significantly higher relative FDG uptake in superior temporal gyrus and hippocampi in patients with ALS, in particular spinal patients. Midbrain hypermetabolism can be considered one of the signatures of ALS and might be related to both motor neuron degeneration and astrocytosis. Functional investigations found reduced neuronal density in pyramidal cells and interneurons in motor and premotor cortices,[19] widespread astrocytosis,[20] and microglial activation in motor cortex and pons.[21] Along with activated microglia and macrophages, a 60% increase in ^{18}F-FDG metabolic rate constant was found in areas of neuroinflammation.[5] During the course of neurodegenerative disorders, dead neurons and axons are replaced by astrocytes filling the

Figure 2 Metabolic differences in controls vs spinal patients and bulbar patients

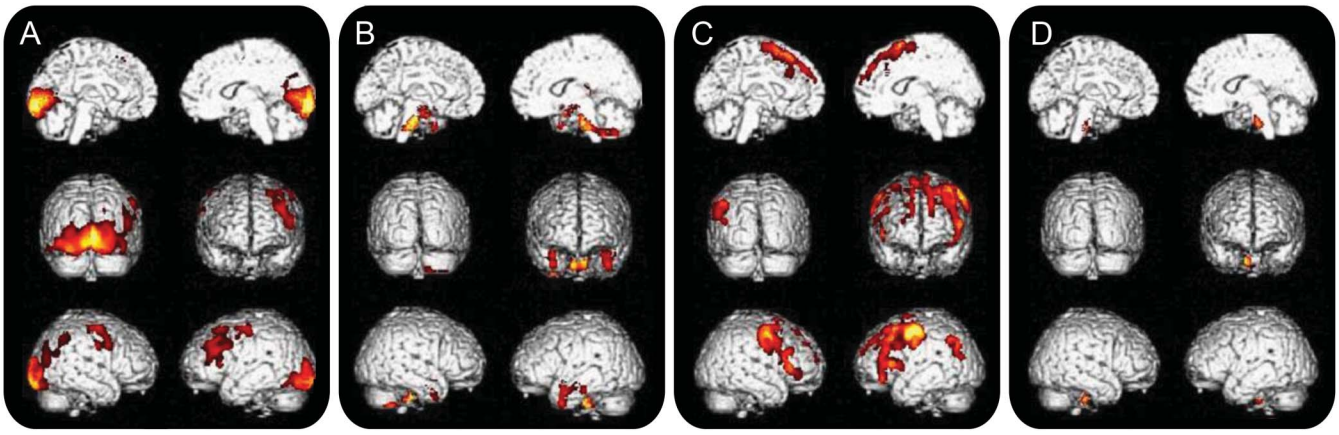

Figure displays regions of significant metabolic differences: (A) hypometabolic regions in spinal patients; (B) hypermetabolic regions in spinal patients; (C) hypometabolic regions in bulbar patients; (D) hypermetabolic regions in bulbar patients. Images are color-graded in terms of *z* values. Talairach coordinates and further details are provided in tables e-1 and e-2.

space left empty by their shrinkage.[22] Several studies reported reactive astrogliosis fanning out from primary motor cortex to the descending white matter tracts and the brainstem.[20,23–25] This strong glial reaction causes proliferation of astrocytes, the main determinant of ^{18}F-FDG uptake in the astrocyte-neuron functional unit.[4] Furthermore, PET studies in ALS found microglia proliferation and astrocytosis in subcortical white matter, pons, and midbrain, suggesting glial cell involvement in the disease.[21,26,27] Astrocytes account for about 50% of glucose consumption at rest[5,28] since glycolytic activity, including anaerobic glycolysis, is higher in glial cells than in neurons, with the former taking up glucose directly from intraparenchymal capillaries. Glutamate-induced glycolysis in astrocytic syncytium provides lactate as substrate for neuronal firing,[29] and in ALS glutamate excess is proportional to the presence of dysarthria and dysphagia.[30] Taken together, these phenomena may result in regions of neuronal degeneration in an increased relative ^{18}F-FDG uptake due to the higher density of astrocytes and microglia in patients with ALS compared to controls.

Besides the midbrain, our study showed relative hypermetabolism in the superior temporal gyrus and hippocampus bilaterally in patients with ALS compared to controls. A recent study demonstrated a significant increase of activated glial cells in primary and supplementary motor and temporal cortex in ALS.[27] The latter region (figure 1B) is immediately adjacent to the white matter tracts containing axonal fibers that run in the corona radiata and ultimately into centrum semiovale connecting cerebral cortex and midbrain. In our study, the degeneration of axons in corticofugal fibers is indirectly suggested by the voxel-wise interregional correlation analysis showing a parallel increase in metabolism in midbrain and white matter tracts connecting the latter to motor cortex in ALS (figure 3). These findings replicate with functional neuroimaging the recently reported

Figure 3 Voxelwise interregional correlation analysis in ALS of midbrain hypermetabolic cluster and ^{18}F-FDG uptake in whole brain

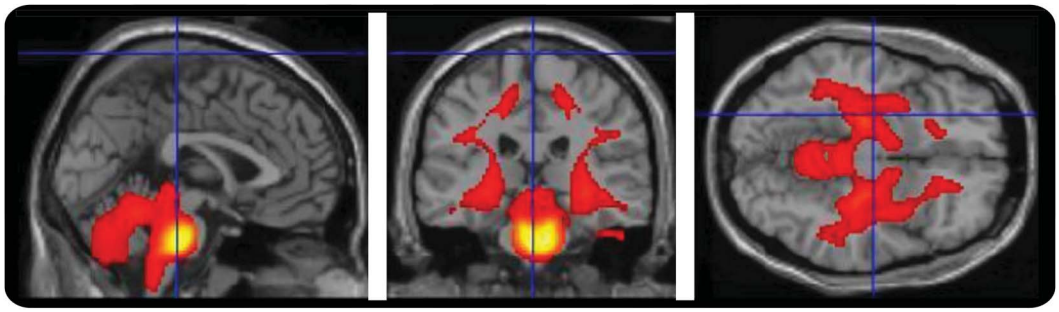

Figure displays regions of metabolically correlated areas at $p < 0.05$ FDR_{corr}. Images are color-graded in terms of *z* values. ^{18}F-FDG = ^{18}F-2-fluoro-2-deoxy-D-glucose; ALS = amyotrophic lateral sclerosis; FDR_{corr} = *p* value corrected for multiple comparisons with the false discovery rate.

Figure 4 Discrimination between controls and patients with amyotrophic lateral sclerosis obtained by generalized linear model

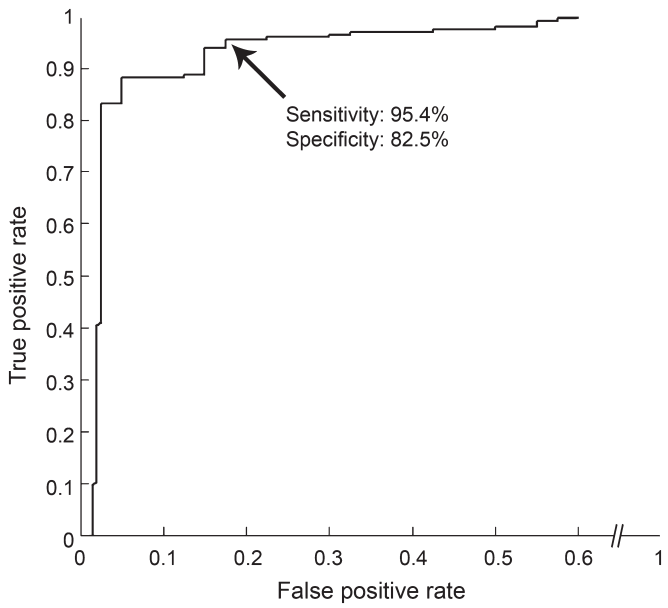

Generalized linear model discriminant model: receiver operating characteristic (ROC) curve. Discriminant capabilities were evaluated by cross-validation using Brodmann areas (BAs): BA6: premotor cortex; BA7: precuneus; BA9 and 10: prefrontal cortex; BA 11 and 47: orbitofrontal cortex; BA13: insula; BA17: primary visual cortex; BA18: visual association cortex; BA21: middle temporal gyrus; BA22: superior temporal gyrus; BA24 and 32: anterior cingulate cortex; BA37: fusiform gyrus; BA39: inferior parietal cortex; BA40: temporoparietal junction; medial temporal lobe: amygdala and hippocampus. Area under ROC curve 94.5%.

selectively reduced fractional anisotropy in corticospinal tracts.[31] On the other hand, the partial volume effect associated with the relatively low spatial resolution of PET and the possible temporal atrophy in ALS might have caused a smearing of the hypermetabolic signal in white matter bundles into isocenters corresponding to gray matter regions (superior temporal gyrus and hippocampi), resulting in an artifactual topographic mismatch.

The second important result of the study is the capability of a routine analysis of ^{18}F-FDG-PET data to discriminate patients with ALS from controls with a sensitivity of 89% and a specificity of 82.5%. This was further strengthened by the generalized linear model analysis in which a selected number of regions showed an even higher sensitivity (95.4%) with the same specificity (82.5%; figure 4), suggesting a possible value of ^{18}F-FDG-PET in correctly identifying patients relative to healthy persons. Furthermore, the characteristic pattern of hypermetabolism and hypometabolism found in patients with ALS and the high discrimination accuracy associated with a specific set of regions involved in this pattern suggest a prospective value of ^{18}F-FDG-PET in differentiating ALS from other pathologic conditions.[32] In this respect, studies including diseased controls, in particular ALS-mimic syndromes, as well as longitudinal studies assessing the prognostic value of the methodology, are needed to further test the clinical value of ^{18}F-FDG-PET in ALS.

This very high sensitivity, equal or superior to that achieved when investigating severe Alzheimer disease,[33,34] is seldom obtained by functional neuroimaging, often due to the statistical limitations associated with having a small number of participants. This restriction is usually overcome by multicenter studies in which large patient cohorts are recruited but in which images originating from different cameras have to be normalized and interpolated. In the present study, the largest ALS ^{18}F-FDG-PET investigation performed so far, the size of the patient and control samples allowed for high accuracy to be reliably obtained. Also, we applied the strict statistical constraint of leave-one-out cross-validation. In fact, cross-validation evaluates the discriminant capability of the statistical model, assessing how the results could be generalized to independent data. Without cross-validation, the overfitting (the adaptation to characteristics peculiar to the sample) could induce overestimation of model accuracy and misclassification of independent samples. Leave-one-out technique classifies each participant by a model fitted to all remaining participants, creating a virtually independent validation set with the same number of observations as the original sample. Cross-validation prevents the predictive model from being forced by data and is of paramount importance in neuroimaging, in which comparison groups are difficult and costly to recruit. Similar discrimination values in ALS were recently obtained by more invasive CSF analyses, although in smaller patient cohorts.[2,35] Furthermore, the accuracy of the present study is superior to the accuracy of the state-of-the-art and time-consuming MRI analyses, often not feasible in the presence of major motor, respiratory, and psychological disability.[3] For this reason, many of the recruited patients could not be investigated by MRI, preventing a valuable comparison of functional and structural findings. On the other hand, the relatively simple analysis protocol, taking a few minutes and based on freeware along with routine ^{18}F-FDG-PET scan, might render this methodology easily accessible to most nuclear medicine departments.

We did not perform a systematic independent interregional correlation analysis covarying ^{18}F-FDG-PET uptake by the values of hypometabolic clusters. Severe anatomical damage of primary motor cortex, corpus callosum, and corticospinal tract degeneration results in extramotor neuronal loss or thinning in frontotemporal and parietal regions, as described by surface-based morphometry and diffusion tensor MRI studies,[36–38] and is associated with regional hypometabolism. In this respect, investigating the networks

underlying the metabolic deficits would not have added relevant information to the current knowledge about the spreading of hypometabolism associated with neuronal damage in ALS.

We acknowledge that the use of a control group with a PET scan negative for oncologic disease is a suboptimal solution with respect to a group of healthy volunteers. However, the control group was specifically set up for this study, strict exclusion criteria were applied, and the same injection/acquisition/reconstruction protocols and scanner were used for both patients and controls. This is of utmost importance in neuroimaging studies, in which the number of potential confounding variables has to be reduced as much as possible. On the other hand, including a control group of neurologically normal participants undergoing PET scan for other reasons prevents healthy individuals from being exposed to radiation.

The need for reliable biomarkers for ALS has been advocated and various potential candidates have been identified.[39] The possible contribution of the widely available ^{18}F-FDG-PET technique in identifying disease progression and suggesting the most appropriate diagnostic algorithm lies in establishing definite metabolic patterns for ALS subgroups (i.e., bulbar and spinal variants). Studies comparing patients with ALS to patients with ALS-mimic syndromes, such as cervical myelopathy, and motor neuron disease variants, such as primary lateral sclerosis and Kennedy disease, are needed to better define the sensitivity and specificity of ^{18}FDG-PET in the diagnosis of ALS. Longitudinal studies will also be needed to investigate not only the neuroradiologic course of the disease (as compared to the natural one) but also the predictive value of ^{18}F-FDG-PET in disclosing the regional involvement before the dissemination of symptoms. The effect of therapeutic agents could also be evaluated at a presymptomatic stage in familial forms, helping to select the more appropriate therapy.

AUTHOR CONTRIBUTIONS

Study concept and design: Pagani, Chiò, Valentini, Cistaro. Acquisition of data: Calvo, Moglia, Bertuzzo, Fania. Analysis and interpretation of data: Pagani, Chiò, Öberg, Nobili, Bertuzzo, Morbelli, De Carli, Fania, Cistaro. Drafting/revising the manuscript for content: Pagani, Chiò, Nobili. Critical revision of the manuscript for important intellectual content: Pagani, Chiò, Valentini, Calvo, Morbelli, De Carli, Cistaro. Obtaining funding: Chiò. Administrative, technical, and material support: Pagani, Chiò, Valentini, Öberg, Nobili, Calvo, Moglia, Morbelli, De Carli, Fania, Cistaro. Study supervision or coordination: Pagani, Chiò, Valentini, Cistaro.

ACKNOWLEDGMENT

The authors thank the patients and the non-neurologic controls for participating in the study as well as the technician of IRMET S.p.A for providing assistance and making the investigations possible.

STUDY FUNDING

This work was supported in part by Compagnia di San Paolo, Programma Neuroscienze 2008–2009, Ministero della Salute (Ricerca Sanitaria Finalizzata, 2010, grant RF-2010-2309849); European Community's Health Seventh Framework Programme (FP7/2007-2013 under grant agreement 259867).

DISCLOSURE

M. Pagani serves on the editorial board of the *European Journal of Nuclear Medicine and Molecular Imaging*, *The Open Nuclear Medicine Journal*, and the *Journal of Psychology and Psychotherapy Research*. A. Chiò serves on the editorial advisory board of *Amyotrophic Lateral Sclerosis*; has received research support from Italian Ministry of Health (Ricerca Finalizzata), Regione Piemonte (Ricerca Finalizzata), University of Torino, Federazione Italiana Giuoco Calcio, Fondazione Vialli e Mauro onlus, and European Commission (Health Seventh Framework Programme); and serves on scientific advisory boards for Biogen Idec and Cytokinetics. M. Valentini and J. Öberg report no disclosures relevant to the manuscript. F. Nobili serves on the editorial board of the *Quarterly Journal of Nuclear Medicine and Molecular Imaging*. He has received research support from E.U. FP-7 multicenter study on nilvadipine in mild to moderate Alzheimer disease and E.U. Innovative Medical Initiatives (IMI): Pharmacog WP-5. A. Calvo has received research support from Italian Ministry of Health (Ricerca Finalizzata). C. Moglia and D. Bertuzzo report no disclosures relevant to the manuscript. S. Morbelli serves on the editorial board of the *American Journal of Nuclear Medicine and Molecular Imaging* and the *World Journal of Radiology*. F. De Carli, P. Fania, and A. Cistaro report no disclosures relevant to the manuscript. Go to Neurology.org for full disclosures.

Received November 25, 2013. Accepted in final form June 17, 2014.

REFERENCES

1. Brooks BR, Miller RG, Swash M, et al. El Escorial revisited: revised criteria for the diagnosis of amyotrophic lateral sclerosis. Amyotroph Lateral Scler Other Motor Neuron Disord 2000;1:293–299.
2. Pasinetti GM, Ungar LH, Lange DJ, et al. Identification of potential CSF biomarkers in ALS. Neurology 2006;66:1218–1222.
3. Filippini N, Douaud G, Mackay CE, et al. Corpus callosum involvement is a consistent feature of amyotrophic lateral sclerosis. Neurology 2010;75:1645–1652.
4. Magistretti PJ. Cellular bases of functional brain imaging: insights from neuron–glia metabolic coupling. Brain Res 2000;886:108–112.
5. Schroeter M, Dennin MA, Walberer M, et al. Neuroinflammation extends brain tissue at risk to vital peri-infarct tissue: a double tracer [11C]PK11195- and [18F]FDG-PET study. J Cereb Blood Flow Metab 2009;29:1216–1225.
6. Claassen DO, Josephs KA, Peller PJ. The stripe of primary lateral sclerosis: focal primary motor cortex hypometabolism seen on fluorodeoxyglucose F18 positron emission tomography. Arch Neurol 2010;67:122–125.
7. Dalakas MC, Hatazawa J, Brooks RA, et al. Lowered cerebral glucose utilization in amyotrophic lateral sclerosis. Ann Neurol 1987;22:580–586.
8. Peavy GM, Herzog AG, Rubin NP, et al. Neuropsychological aspects of dementia of motor neuron disease: a report of two cases. Neurology 1992;42:1004–1008.
9. Ludolph AC, Langen KJ, Regard M, et al. Frontal lobe function in amyotrophic lateral sclerosis: a neuropsychologic and positron emission tomography study. Acta Neurol Scand 1992;85:81–89.
10. Cistaro A, Valentini MC, Chiò A, et al. Brain hypermetabolism in amyotrophic lateral sclerosis: a FDG PET study in ALS of spinal and bulbar onset. Eur J Nucl Med Mol Imaging 2012;39:251–259.
11. Varrone A, Asenbaum S, Vander Borght T, et al. EANM procedure guidelines for PET brain imaging using

[18F]FDG, version 2. Eur J Nucl Med Mol Imaging 2009;36:2103–2110.
12. Morbelli S, Rodriguez G, Mignone A, et al. The need of appropriate brain SPECT templates for SPM comparisons. Q J Nucl Med Mol Imaging 2008;52:89–98.
13. Morbelli S, Drzezga A, Perneczky R, et al. Resting metabolic connectivity in prodromal Alzheimer's disease. A European Alzheimer Disease Consortium (EADC) project. Neurobiol Aging 2012;33:2533–2550.
14. Cistaro A, Pagani M, Montuschi A, et al. The metabolic signature of C9ORF72-related ALS: FDG PET comparison with non-mutated patients. Eur J Nucl Med Mol Imaging 2014;41:844–852.
15. Phukan J, Elamin M, Bede P, et al. The syndrome of cognitive impairment in amyotrophic lateral sclerosis: a population–based study. J Neurol Neurosurg Psychiatry 2012;83:102–108.
16. Bede P, Bokde A, Elamin M, et al. Grey matter correlates of clinical variables in amyotrophic lateral sclerosis (ALS): a neuroimaging study of ALS motor phenotype heterogeneity and cortical focality. J Neurol Neurosurg Psychiatry 2013;84:766–773.
17. Bede P, Bokde AL, Byrne S, et al. Multiparametric MRI study of ALS stratified for the C9orf72 genotype. Neurology 2013;81:361–369.
18. Verstraete E, Veldink JH, Hendrikse J, Schelhaas HJ, van den Heuvel MP, van den Berg LH. Structural MRI reveals cortical thinning in amyotrophic lateral sclerosis. J Neurol Neurosurg Psychiatry 2012;83:383–388.
19. Lloyd CM, Richardson MP, Brooks DJ, et al. Extramotor involvement in ALS: PET studies with the GABA(A) ligand [(11)C]flumazenil. Brain 2000;123:2289–2296.
20. Yamanaka K, Chun SJ, Boillee S, et al. Astrocytes as determinants of disease progression in inherited amyotrophic lateral sclerosis. Nat Neurosci 2008;11:251–253.
21. Turner MR, Cagnin A, Turkheimer FE, et al. Evidence of widespread cerebral microglial activation in amyotrophic lateral sclerosis: an [11C](R)-PK11195 positron emission tomography study. Neurobiol Dis 2004;15:601–609.
22. Marik J, Ogasawara A, Martin–McNulty B, et al. PET of glial metabolism using 2-18F-fluoroacetate. J Nucl Med 2009;50:982–990.
23. Kushner PD, Stephenson DT, Wright S. Reactive astrogliosis is widespread in the subcortical white matter of amyotrophic lateral sclerosis brain. J Neuropathol Exp Neurol 1991;50:263–277.
24. Barbeito LH, Pehar M, Cassina P, et al. A role for astrocytes in motor neuron loss in amyotrophic lateral sclerosis. Brain Res Brain Res Rev 2004;47:263–274.
25. Philips T, Robberecht W. Neuroinflammation in amyotrophic lateral sclerosis: role of glial activation in motor neuron disease. Lancet Neurol 2011;10:253–263.
26. Johansson A, Engler H, Blomqvist G, et al. Evidence for astrocytosis in ALS demonstrated by [11C](L)–deprenyl–D2 PET. J Neurol Sci 2007;255:17–22.
27. Corcia P, Tauber C, Vercoullie J, et al. Molecular imaging of microglial activation in amyotrophic lateral sclerosis. PLoS One 2012;7:e52941.
28. Nehlig A, Coles J. Cellular pathways of energy metabolism in the brain: is glucose used by neurons or astrocytes? Glia 2007;55:1238–1250.
29. Pellerin L, Magistretti PJ. Sweet sixteen for ANLS. J Cereb Blood Flow Metab 2012;32:1152–1166.
30. Pioro EP, Majors AW, Mitsumoto H, et al. ^{1}H–MRS evidence of neurodegeneration and excess glutamate + glutamine in ALS medulla. Neurology 1999;53:71–79.
31. Sage CA, Peeters RR, Görner A, et al. Quantitative diffusion tensor imaging in amyotrophic lateral sclerosis. Neuroimage 2007;34:486–499.
32. Traynor BJ, Codd MB, Corr B, Forde C, Frost E, Hardiman O. Amyotrophic lateral sclerosis mimic syndromes: a population–based study. Arch Neurol 2000; 57:109–113.
33. Shao J, Myers N, Yang Q, et al. Prediction of Alzheimer's disease using individual structural connectivity networks. Neurobiol Aging 2012;33:2756–2765.
34. Kakimoto A, Kamekawa Y, Ito S, et al. New computer-aided diagnosis of dementia using positron emission tomography: brain regional sensitivity-mapping method. PLoS One 2011;6:e25033.
35. Mitchell RM, Freeman WM, Randazzo WT, et al. A CSF biomarker panel for identification of patients with amyotrophic lateral sclerosis. Neurology 2009;72:14–19.
36. Schuster C, Kasper E, Dyrba M, et al. Cortical thinning and its relation to cognition in amyotrophic lateral sclerosis. Neurobiol Aging 2014;35:240–246.
37. Pettit LD, Bastin ME, Smith C, Bak TH, Gillingwater TH, Abrahams S. Executive deficits, not processing speed relates to abnormalities in distinct prefrontal tracts in amyotrophic lateral sclerosis. Brain 2013;136: 3290–3304.
38. Sarro L, Agosta F, Canu E, et al. Cognitive functions and white matter tract damage in amyotrophic lateral sclerosis: a diffusion tensor tractography study. AJNR Am J Neuroradiol 2011;32:1866–1872.
39. Turner MR, Kiernan MC, Leigh PN, et al. Biomarkers in amyotrophic lateral sclerosis. Lancet Neurol 2009;8: 94–109.